Twisted magnetization states near the compensation temperature of Fe/Gd multilayers: Anisotropy and surface-termination effects

Y. Choi,[1,2] D. Haskel,[2] A. Cady,[2] J. C. Lang,[2] D. R. Lee,[2] G. Srajer,[2] J. S. Jiang,[3] and S. D. Bader[3]
[1]*Department of Materials Science and Engineering, Northwestern University, Evanston, Illinois 60208, USA*
[2]*Advanced Photon Source, Argonne National Laboratory, Argonne, Illinois 60439, USA*
[3]*Materials Science Division, Argonne National Laboratory, Argonne, Illinois 60439, USA*
(Received 10 June 2005; revised manuscript received 28 October 2005; published 1 May 2006)

Inhomogeneous magnetization depth profiles in antiferromagnetically coupled Fe/Gd multilayers are investigated using x-ray magnetic circular dichroism (XMCD) measurements. Spin configurations are studied as a function of temperature and applied field on two multilayers with different termination layers. We place particular emphasis on the vicinity of the ferrimagnetic compensation temperature (T_{Comp}), where the Gd and Fe magnetizations are equal but opposite. While away from T_{Comp} the spin configurations are dictated by the presence of surface- and bulk-twisted states, unusual field dependence is observed near T_{Comp}. We used micromagnetic simulations to show that the unusual observed phenomena near T_{Comp} are due to a small uniaxial anisotropy in the Fe layers, whose influence on the spin configurations becomes apparent only near T_{Comp}. The simulations also show the onset of the surface- and bulk-twisted phases at temperatures below and above T_{Comp} in agreement with the experimental XMCD data.

DOI: 10.1103/PhysRevB.73.174401 PACS number(s): 75.70.−i, 75.25.+z, 61.10.−i

I. INTRODUCTION

Magnetic multilayers have been the topic of intense research as they exhibit a myriad of novel magnetic phenomena arising from direct exchange across interfaces or indirect layer coupling through nominally nonmagnetic spacers. One of the most well-known phenomena due to the direct magnetic coupling is exchange bias between ferromagnetic and antiferromagnetic layers, which causes a field shift in the hysteresis loop of the ferromagnetic layer.[1] In some artificial antiferromagnetic multilayers with indirect coupling, the competition between the exchange, Zeeman, and anisotropy interactions can lead to a spin-flop transition, resulting in canting of the sublattice magnetization.[2] In these systems, surface effects play an important role. The surface spin-flop transition occurs at lower fields than the bulk transition and depends on the number of layers.[3]

Fe/Gd multilayers have been extensively used as model systems as they display a wide variety of magnetic configurations easily tunable by temperature and field. While Fe and Gd layers couple antiferromagnetically at their interfaces (hence forming an artificial ferrimagnet), the different temperature dependences of the Fe and Gd magnetizations lead to a true antiferromagnet at the compensation temperature T_{Comp}, where the Gd and Fe magnetizations are equal in magnitude but opposite in direction. Away from T_{Comp} the phase diagram consists of aligned phases at low fields (exchange-dominated) and twisted phases at high fields (exchange-Zeeman competition).[4] The twisted phases are characterized as surface- and bulk-twists, depending on whether the twist nucleates at the surface or interior of the multilayer.[4,5]

Evidence for twisted states of spins in Fe/Gd multilayers comes from magnetoresistive,[6] polarized neutron scattering,[7,8] x-ray resonant magnetic scattering,[9] magneto-optical Kerr effect,[8] magnetometry,[6–10] and x-ray magnetic circular dichroism (XMCD) measurements.[11,12] However, the direct experimental observation of the surface-twisted state has been challenging due to the difficulty in probing surface and bulk states in the same measurement.

Previously, surface- and bulk-twisted states have been observed using element-specific XMCD loops with varying penetration depth in order to separate surface and bulk signals.[12] However, a Nb capping layer prevented the measurement of surface-sensitive Fe loops, allowing only Fe bulk loops, and Gd surface and bulk loops, to be measured.[12] As discussed below, the ability to also probe the Fe surface's magnetism is important, especially for Fe-terminated multilayers where Fe end layers drive the nucleation of a surface twist.

In this paper, we present results obtained from Fe/Gd multilayers prepared with an Al capping layer that permits the study of both the Fe and Gd surface states. We studied two multilayers with different termination layers since the transition from the Gd and Fe aligned to the twisted state can be modified by the termination layers (top and bottom) of the stack. From element-specific XMCD hysteresis loop measurements at different x-ray penetration depths, we observed surface/bulk-twisted spin states as previously reported. In addition, we found that the often neglected anisotropy contribution[4,5] plays an important role near T_{Comp}. For the Fe-terminated multilayer near T_{Comp}, we observed field shifting and lack of sign reversal in the element-specific XMCD hysteresis loops. These phenomena can be explained by the effect of a weak uniaxial anisotropy in the Fe layers, based on the comparison between micromagnetic simulations and experimental results. We found that the weak anisotropy plays an important role near T_{Comp}, while its importance decreases at temperatures away from T_{Comp}. Thus the diminished net Zeeman energy contribution near T_{Comp} results in a magnetic ground state that is highly susceptible to small interactions such as a small uniaxial anisotropy.

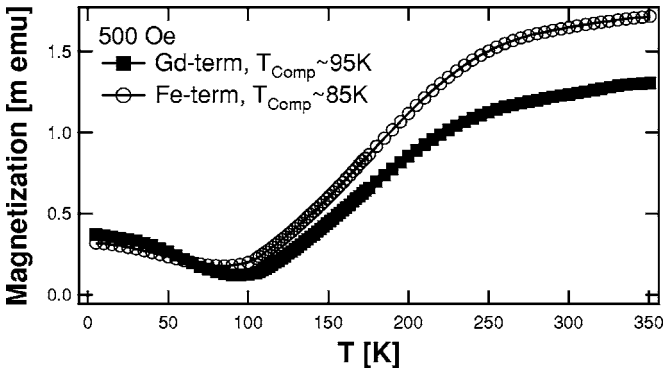

FIG. 1. SQUID magnetization measurements on the Fe-terminated and Gd-terminated [Fe/Gd] multilayers. The ferrimagnetic compensation temperatures are approximately 85 and 95 K for the Fe- and Gd-terminated samples, respectively. The applied field is 500 Oe.

II. EXPERIMENTAL PROCEDURES

A. Samples

Two multilayer films, about 8×8 mm^2 in size, were prepared in vacuum by sputtering Fe and Gd onto a Si substrate with Al buffer (100 Å) and cap (50 Å) layers. The base pressure of our magnetron-sputtering chamber was about 1.8×10^{-8} Torr with Fe and Gd sputtering rates of 1 to 2 Å/s. The Fe-terminated multilayer sample has the sequence $[\mathrm{Fe}(35\ \text{Å})/\mathrm{Gd}(50\ \text{Å})]_{15}/\mathrm{Fe}(35\ \text{Å})$, and the Gd-terminated multilayer is $[\mathrm{Gd}(50\ \text{Å})/\mathrm{Fe}(35\ \text{Å})]_{15}/\mathrm{Gd}(50\ \text{Å})$.

Superconducting quantum interference device (SQUID) magnetometry measurements were performed as a function of temperature as shown in Fig. 1. The initial decrease in magnetization with increasing temperature is due to reduction of the Gd moment ($T_C=293$ K), while the Fe moment is nearly unchanged ($T_C=1043$ K). The minima of the M vs T curves in Fig. 1 slightly differ for the two samples since the Fe-terminated sample has one less Gd layer than the Gd-terminated sample, thus a lower T_{Comp} [$M_S(\mathrm{Gd})=2020$ emu/cm^3, $M_S(\mathrm{Fe})=1720$ emu/cm^3].

X-ray reflectivity measurements were performed on the Fe- and Gd-terminated multilayers in order to determine structural parameters for micromagnetic simulations. For each multilayer, the reflectivity measurements were performed at a nonresonant (7.0 keV) and a resonant energy (7.245 keV, near the Gd L_3 edge). The contrast in optical constants between Gd and Fe is low at the nonresonant energy, and thus the reflectivity measurements were repeated at the resonant energy where the contrast becomes larger. The atomic scattering factors of Gd were obtained via a Kramers-Krönig transform of Gd absorption spectra measured on the samples.[13–15] For each multilayer, the two reflectivity curves measured at the two energies were fitted simultaneously with one set of parameters using Parratt's recursive formula for x-ray reflectivity.[16] From the fit of x-ray reflectivity data, Fe/Gd bilayer thicknesses are 85.3 and 87.6 Å for the Fe-terminated and Gd-terminated samples, respectively. The fitted interface roughnesses were $\sigma_{\mathrm{Fe/Gd}}=8.1$ Å and $\sigma_{\mathrm{Gd/Fe}}=4.8$ Å for the Fe-terminated film, and $\sigma_{\mathrm{Fe/Gd}}=5.2$ Å and $\sigma_{\mathrm{Gd/Fe}}=3.9$ Å for the Gd-terminated film.

B. Element-specific hysteresis loop measurements

The x-ray magnetic circular dichroism (XMCD) technique was used for a layer-specific study of the Gd and Fe layer magnetizations. With the incident x-ray energy tuned to a resonance, XMCD measures the difference in absorption between left- and right-circularly polarized x rays. Element-specific XMCD signals are proportional to the projection of the magnetization vector **M** along the x-ray wave vector **k**. Using this technique, element-specific determination of the spatially averaged magnetization can be achieved.[17]

The x-ray measurements were performed at the 4-ID-D beamline of the Advanced Photon Source at Argonne National Laboratory. A diamond (111) quarter-wave plate operated in Bragg transmission geometry was used to produce the circularly polarized x rays.[18] The sample was placed inside a closed-cycle He refrigerator mounted on a diffractometer. An electromagnet was mounted externally to the cryostat to apply a magnetic field parallel to the sample surface and coplanar with the incident x-ray wave vector and sample surface normal.

Element-specific hysteresis loops were measured by recording XMCD signals in fluorescence geometry as a function of the applied field at the Fe K and Gd L_3 absorption edges. A cylindrically bent Laue analyzer crystal[19] was placed in front of a NaI scintillation detector in order to reduce undesired background from scattered x rays and irrelevant fluorescence radiation. In this paper, the term XMCD signal is defined as the asymmetry ratio, $(I^+-I^-)/(I^++I^-)$ where $I^{+,-}$ are the measured fluorescence intensities for the two opposite helicities of the incoming x rays. For each multilayer, Fe-specific XMCD hysteresis loops were measured with x-ray energy at 7.112 keV (Fe K edge, near the first inflection point of absorption spectrum) and Gd-specific XMCD hysteresis loops at 7.247 keV (Gd L_3 edge, near the top of near-edge absorption peak). The selected energies are where the maximum magnetic circular dichroic signals were observed. The sample was cooled to 10 K in zero field, and the XMCD hysteresis loops were measured at temperatures ranging from 10 to 250 K.

For surface- vs bulk-layer sensitivity, the XMCD hysteresis loops were measured at two different x-ray incident angles. At each energy, the first set of measurements was performed at a grazing incident angle ($\theta=0.355°$), and the second set was performed at a higher incident angle ($\theta=5°$). At the high angle, the incoming x rays penetrate through all the layers and thus probe the bulk magnetic properties. The low angle was chosen so that the x rays would penetrate only the near-surface layers, and thus the low-angle measurement would serve as a near-surface magnetization probe. Based on the tabulated values,[20] at $E=7.112$ and 7.247 keV, $\theta=0.355°$ is near the critical angles for total external reflection $\theta_C(\mathrm{Fe})$ and $\theta_C(\mathrm{Gd})$. With the incident energy $E=7.112$ keV (Fe K), $\theta_C(\mathrm{Fe})=0.335°$ and $\theta_C(\mathrm{Gd})=0.374°$ so that $\theta_C(\mathrm{Fe})<0.355°<\theta_C(\mathrm{Gd})$. With $E=7.247$ keV (Gd L_3), $\theta_C(\mathrm{Fe})=0.406°$ and $\theta_C(\mathrm{Gd})=0.306°$ so that $\theta_C(\mathrm{Gd})<0.355°<\theta_C(\mathrm{Fe})$.

Figure 2 presents the electric field intensity profiles inside the multilayers as calculated using Parratt's recursive for-

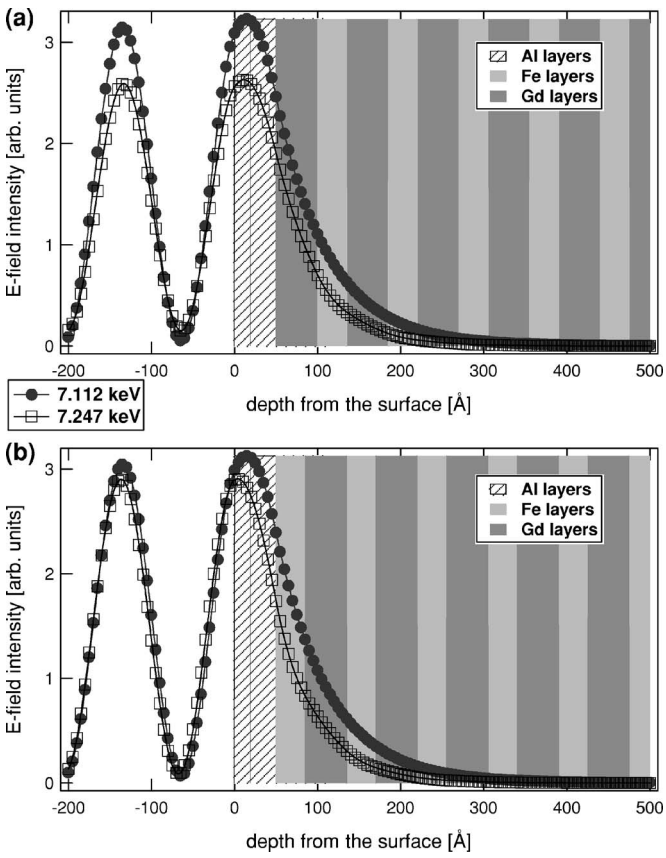

FIG. 2. Electric field intensity profiles inside the multilayers at a grazing incident angle of 0.355°. Positive values for the depth from the surface correspond to inside the multilayers, and negative values correspond to air. The first 50 Å corresponds to an Al capping layer. The incoming x-ray energies are 7.112 (Fe K) and 7.247 (Gd L_3) keV. Only the top half of the multilayer is shown for each case. (a) Gd-terminated sample and (b) Fe-terminated sample.

mula with the experimentally obtained x-ray optical constants for Gd and Fe. The attenuation length is calculated to be less than 1.5 bilayers at the incident angle $\theta=0.355°$ for all cases considered here (two energies and two samples). Using these profiles, the integrated electric field intensity for each layer can be calculated, and the integrated intensity from the first Fe(Gd) layer was 3.84(5.56) times larger than that from the second Fe(Gd) layer. Based on this calculation, we concluded that the measured Fe $K\alpha$ and Gd $L\alpha$ fluorescence radiation at $\theta=0.355°$ originates mainly from the first Fe/Gd bilayer. The calculated probing depth at the low incidence angle can be considered as an upper limit since the fluorescence energy is lower than the incident energy. At the high incidence angle of 5° the x-ray intensity inside the multilayer is determined by the linear absorption coefficient. This yields a relatively uniform intensity profile inside the multilayer, with only about 20% intensity decrease at the Fe resonance and 40% decrease at the Gd resonance at the bottom of the multilayer stack.

C. Micromagnetic simulation

Spin configurations in the Fe/Gd multilayers were modeled using LLG Micromagnetics Simulator.[21] The Fe-terminated and the Gd-terminated samples were modeled separately. For the Fe-terminated sample ($[\mathrm{Fe}(35\ \text{Å})/\mathrm{Gd}(50\ \text{Å})]_{15}/\mathrm{Fe}(35\ \text{Å})$, the total simulation volume was $50\times50\times0.131\ \mu\mathrm{m}^3$. The simulation cell size was $50\times50\times0.0005\ \mu\mathrm{m}^3$, and each Fe and Gd layer was sliced into 7 and 10 sublayers, respectively. The same cell size was used for the Gd-terminated sample ($[\mathrm{Gd}(50\ \text{Å})/\mathrm{Fe}(35\ \text{Å})]_{15}/\mathrm{Gd}(50\ \text{Å})$) with $50\times50\times0.1325\ \mu\mathrm{m}^3$ total simulation volume. In these simulations, the magnetic configuration is assumed to be uniform within the layer plane, allowing each multilayer to be approximated as a discrete chain of spins. An equilibrium configuration was assumed when the maximum change in $|M/M_S|$ between successive iterations was less than 10^{-9}; restricting the convergence criteria further did not affect the simulation output.

For the Fe layers, the saturation moment M_S was $1700\ \mathrm{emu/cm}^3$, and the layer exchange J_{Fe} was $2.1\ \mu\mathrm{erg/cm}$. It was assumed that the changes in these Fe magnetic parameters were negligible from 20 to 300 K. While the anisotropy in the Gd layers was assumed to be negligible, a uniaxial magnetic anisotropy was included for the Fe layers. Later, in order to match the simulation data with the experimental results, the magnitude and direction of the Fe anisotropy were varied. For the Gd layers, J_{Gd} was calculated based on the mean field theory expression $J=3k_BT_C/2zS(S+1)$ with reduced $T_C(\mathrm{Gd})=220$ K. The $T_C(\mathrm{Gd})$ was determined experimentally by XMCD measurements on a similarly grown ($[\mathrm{Gd}(50\ \text{Å})/\mathrm{Fe}(15\ \text{Å})]_{15}$) multilayer.[15] J_{Gd} was calculated to be $0.054\ \mu\mathrm{erg/cm}$, and the antiferromagnetic coupling between Gd and Fe was chosen to be $J_{\mathrm{Fe/Gd}}=-(J_{\mathrm{Fe}}+J_{\mathrm{Gd}})/2=-1.077\ \mu\mathrm{erg/cm}$. For more realistic simulations, roughness and interfacial effects[15] in Gd layers need to be included. However, since the contributions from these effects are not easily quantifiable, the value of $J_{\mathrm{Fe/Gd}}$ used here can be considered as an *effective* interlayer exchange constant in which any roughness and interfacial effects are implicitly included. The saturation moment of Gd at 0 K was reduced by 30% from its bulk value in order to reproduce the XMCD hysteresis experimental results as reported similarly in experimental and theoretical works by others.[4,8,9,22]

Temperature changes were modeled by changing the value of $M_S(\mathrm{Gd})$. It was assumed that the temperature dependence of the Gd saturation moment is the same for the current samples and the above-mentioned $[\mathrm{Gd}(50\ \text{Å})/\mathrm{Fe}(15\ \text{Å})]_{15}$ multilayer that remains in the Gd-aligned phase from 20 to 300 K. On this multilayer, the Gd L_2 XMCD peaks were measured from 20 to 300 K, and the temperature dependence of the Gd layer magnetization was approximated by using the integrated areas of the XMCD peaks.[15]

III. RESULTS AND DISCUSSION

A. Fe-terminated sample

Element-specific hysteresis loops from the XMCD measurements on the Fe-terminated sample are shown in Fig. 3. The results in the first and third columns were measured at a grazing incident angle for top-layer sensitivity (labeled "sur-

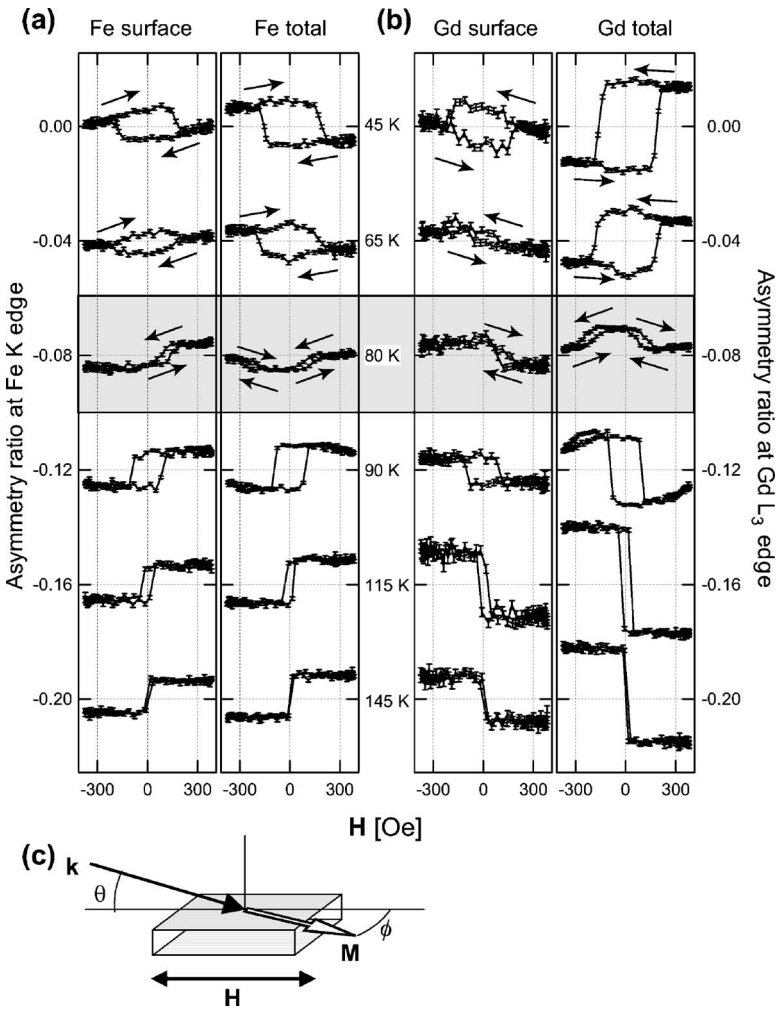

FIG. 3. Element-specific XMCD hysteresis loops from the Fe-terminated sample at the indicated temperatures. The XMCD signal is recorded as an asymmetry ratio as defined in Sec. II B of the text. The first column in each plot shows hysteresis loops for the top layers, and the second column is for the total layers. For clarity, the hysteresis loops are shifted down vertically by multiples of 0.04. The loops at 80 K are shaded to indicate the temperature is near the compensation temperature. The arrows in (a) and (b) indicate the path of the curves. (a) Fe hysteresis loops, (b) Gd hysteresis loops, and (c) experimental geometry. The XMCD signal $\propto \mathbf{k}\cdot\mathbf{M}$, where $\mathbf{k}$ is the incident x-ray wave vector and $\mathbf{M}$ is the sample magnetization (Gd-XMCD $\propto \mathbf{k}\cdot\mathbf{M}_{\mathrm{Gd}}$ and Fe-XMCD $\propto \mathbf{k}\cdot\mathbf{M}_{\mathrm{Fe}}$). The applied field is $\mathbf{H}$, θ is the x-ray incident angle, and ϕ is the in-plane canting angle of the layer magnetization.

face"), and the loops in the other two columns were measured at a high angle (labeled "total") probing the entire multilayer. At each temperature the Gd and Fe XMCD signals have opposite signs indicating antiparallel alignment between the Gd and Fe moments. From the SQUID results (Fig. 1), T_{Comp} is 85 K for this sample. In Fig. 3, the sign of hysteresis loops is reversed between 65 and 90 K in agreement with the SQUID results.

What is noticeable in Fig. 3 is that at 45 K the surface hysteresis loops are tilted, while their total counterparts are not. Since the XMCD signal is proportional to the magnetization projected along the incident x-ray wave vector (XMCD $\propto \mathbf{k}\cdot\mathbf{M}$), the decreased projected magnetization suggests that the surface-layer magnetization is canted away from the field direction, as illustrated in Fig. 3(c). At low temperatures (10 K), the multilayer is in the Gd-aligned state, where the net Gd layer moment $\mathbf{M}_{\mathrm{Gd}}$ (majority component) is parallel to the field, while the net Fe layer moment $\mathbf{M}_{\mathrm{Fe}}$ (minority component) is antiparallel. In contrast to the interior Fe layers, the top Fe layer is coupled to a Gd layer on only one side. Because of this reduced coupling effect, the top Fe layer moment responds more readily to the applied field. As a result, the surface Fe layer magnetization starts to twist toward the applied field resulting in an increase in the net magnetization component ($\mathbf{M}_{\mathrm{Gd}}+\mathbf{M}_{\mathrm{Fe}}$) along the field (thus decreasing the Zeeman energy) at the expense of the increased exchange energy due to the noncollinearity between $\mathbf{M}_{\mathrm{Gd}}$ and $\mathbf{M}_{\mathrm{Fe}}$. Meanwhile, the interior Fe layers are coupled to Gd layers on both sides and thus do not exhibit a twisted magnetization state. The twisting starts from the surface and penetrates at least the top Gd layer as shown in the first hysteresis loops in Fig. 3(b).

As the temperature is increased above T_{Comp}, the sample is in the Fe-aligned state since the net moment of the Fe layers is larger than that of the Gd layers. In this case, the majority component $\mathbf{M}_{\mathrm{Fe}}$ is parallel to the field, while the minority component $\mathbf{M}_{\mathrm{Gd}}$ is antiparallel. At 90 K, the top Fe layer is now aligned parallel to the field, and the twisting does not occur at the surface. Instead, the twisting is now driven by the minority Gd layer moments, and the total hysteresis loops are tilted, while the surface loops are not (bulk twisted state). This bulk twisting is only observed at temperatures slightly above T_{Comp}. At higher temperatures the Fe layer moment becomes dominant compared with the Gd layer moment, thus twisting the majority Fe layer moments becomes unfavorable.

Near T_{Comp}, the XMCD hysteresis loops at 80 K in Fig. 3 show distinctively different features. The surface loops are shifted as if they were biased, and the total hysteresis loops do not change their magnetization directions even as the applied field is reversed. At this temperature, the Gd layer and

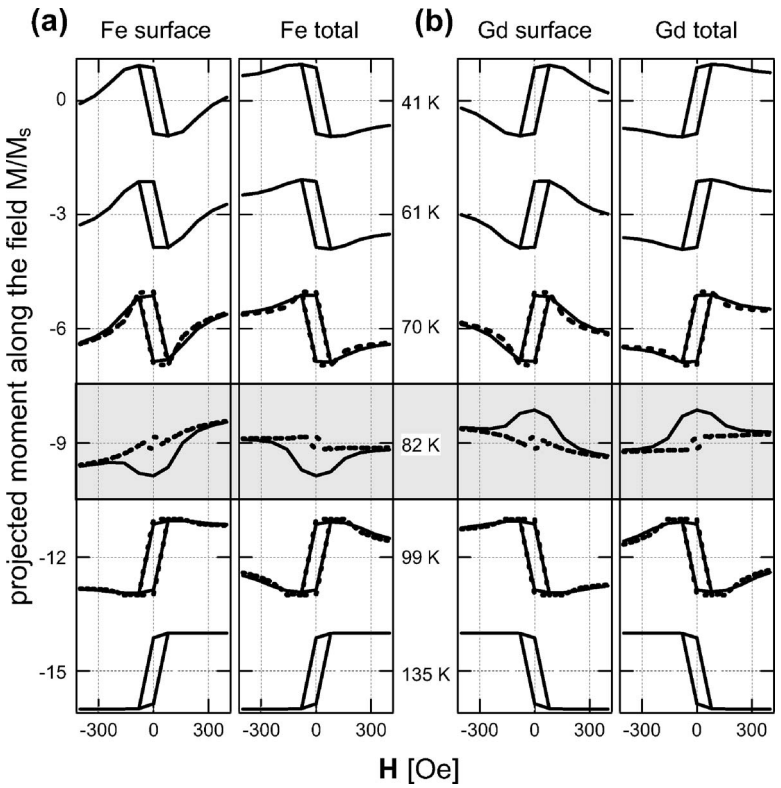

FIG. 4. Element-specific hysteresis loops from the micromagnetic simulations on the Fe-terminated multilayer. The loops are shifted down vertically by multiples of 3 for clarity. The loops at 82 K are shaded to indicate the temperature is near the compensation temperature. For $T=70$, 82, and 99 K, simulation results without the Fe anisotropy are shown as dashed lines for comparison. (a) Fe hysteresis loops. (b) Gd hysteresis loops.

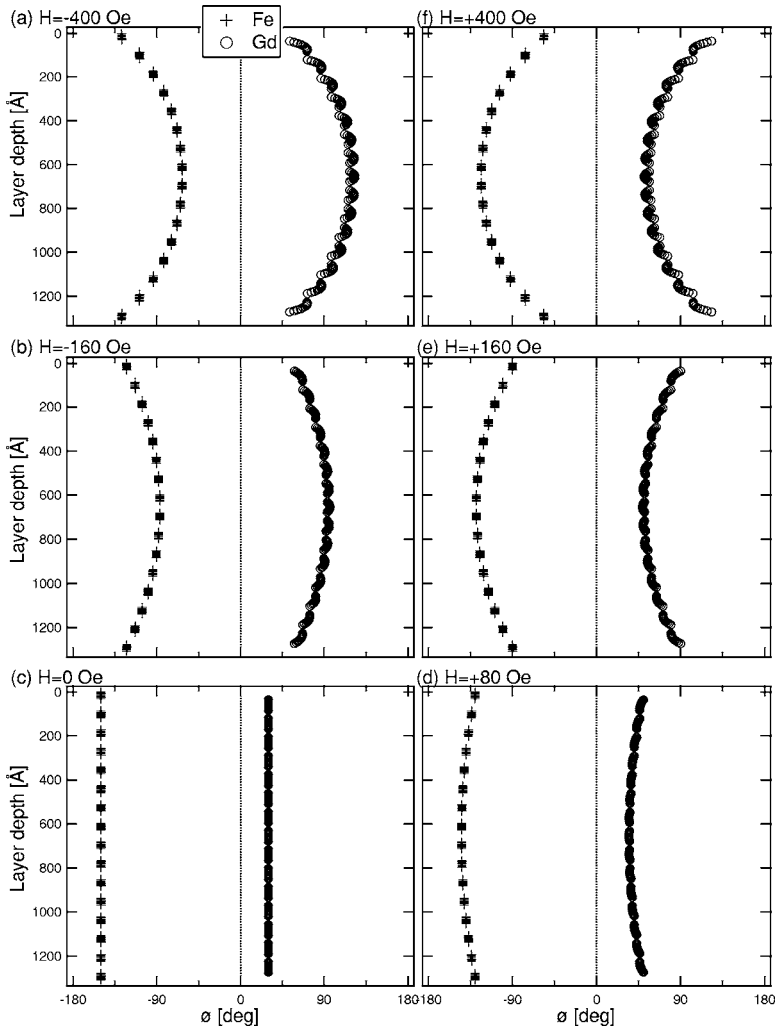

FIG. 5. Simulated spin configurations for the Fe-terminated sample slightly above T_{Comp} ($T=82$ K) at the selected field values as field is swept as in Fig. 4. For each sublayer, the magnetization angle ϕ with respect to the applied field direction ($H\|0°$ or $H\|180°$) is plotted as a function of depth from the surface. The circles represent the Gd moments, and the crosses are for the Fe moments. The uniaxial anisotropy of Fe layers is along $\phi=30°$. (a) At −400 Oe, (b) at −160 Oe, (c) at remanence, (d) at +80 Oe, (e) at +160 Oe, and (f) at +400 Oe.

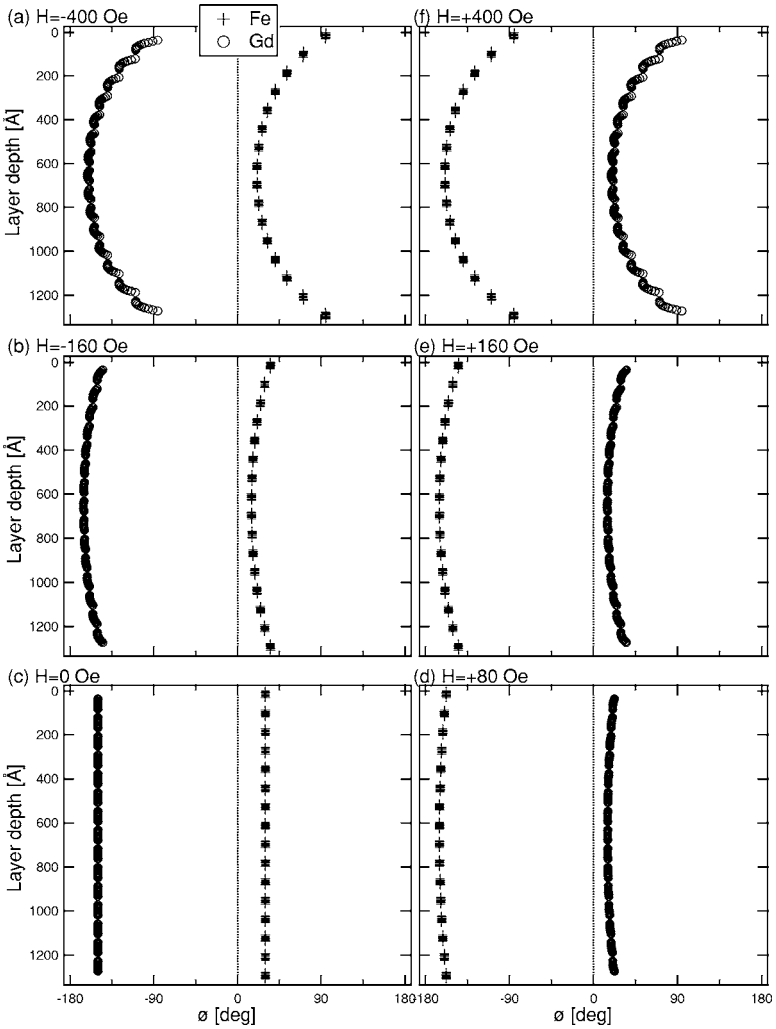

FIG. 6. Simulated spin configurations are shown for the Fe-terminated sample below T_{Comp} (T=41 K) at the selected field values as the field is swept as in Fig. 4. For each sublayer, the magnetization angle ϕ with respect to the applied field direction ($H\|0°$ or $H\|180°$) is plotted as a function of depth from the surface. The circles represent the Gd moments, and the crosses are for the Fe moments. The uniaxial anisotropy of Fe layers is along ϕ=30°. (a) At −400 Oe, (b) at −160 Oe, (c) at remanence, (d) at +80 Oe, (e) at +160 Oe, and (f) at +400 Oe.

the Fe layer moments are comparable to each other in magnitude, and an additional effect may play a role in tipping the energy balance, causing the observed features.

To explore the unusual features near T_{Comp}, micromagnetic simulations were performed. The simulated hysteresis loops for the Fe-terminated sample are shown in Fig. 4. The ground-state configuration was found at each field value, and the normalized local magnetization was calculated by projecting each sublayer spin along the field direction. The first and the third columns in Fig. 4 were obtained by averaging the projected magnetization of the sublayers in the first Fe or Gd layers, respectively. The second and the fourth columns were obtained by averaging magnetization values from all Fe or Gd sublayers, respectively. When comparing the simulated, bulk-averaged loops with experiment one should account for the x-ray intensity profile inside the multilayer sample. For the high incidence angle of 5°, however, the intensity decrease causes negligible effects and was ignored.

Initially, no anisotropy was included in the simulated systems. Magnetic anisotropy contributions are often ignored in Fe/Gd multilayer systems[4,5] because Gd has a very weak magnetic anisotropy and also because the sputtered layers are typically polycrystalline. In this study, when no anisotropy was included, the micromagnetic simulation results were in good agreement with the XMCD experimental results everywhere except near T_{Comp}. As discussed earlier, the measured XMCD hysteresis loops near T_{Comp} show distinctive features, such as field shifting and lack of sign reversal of the loops, and these features could not be reproduced in the simulations, as shown in Fig. 4 (dashed lines at 70, 82, and 99 K). In order to investigate whether the observed features are due to some anisotropy contributions, a uniaxial anisotropy was included in the Fe layers in the micromagnetic simulations. The magnitude and direction of this anisotropy were varied while comparing with the XMCD experimental results. The observed features in the XMCD results (field shifting and lack of sign reversal of the loops) were reproduced by introducing a uniaxial anisotropy of 4700 erg/cm^3 at 30° away from the applied field direction. This anisotropy $\mathbf{K_u}$ corresponds to 10% of the nominal value of the bulk Fe anisotropy. The corresponding anisotropy field is $H=2K_u/M_S$ =5.5 Oe. The anisotropy was relatively weak, so that, away from T_{Comp}, the two simulation sets (with and without the anisotropy) were not significantly different from each other, as shown in Fig. 4 (solid and dashed lines). However, near T_{Comp} the difference between the two simulations is significant.

Based on the simulation results, the spin configurations near T_{Comp} (slightly above T_{Comp}) are visualized in Fig. 5. The observed features in the XMCD measurements in Fig. 3

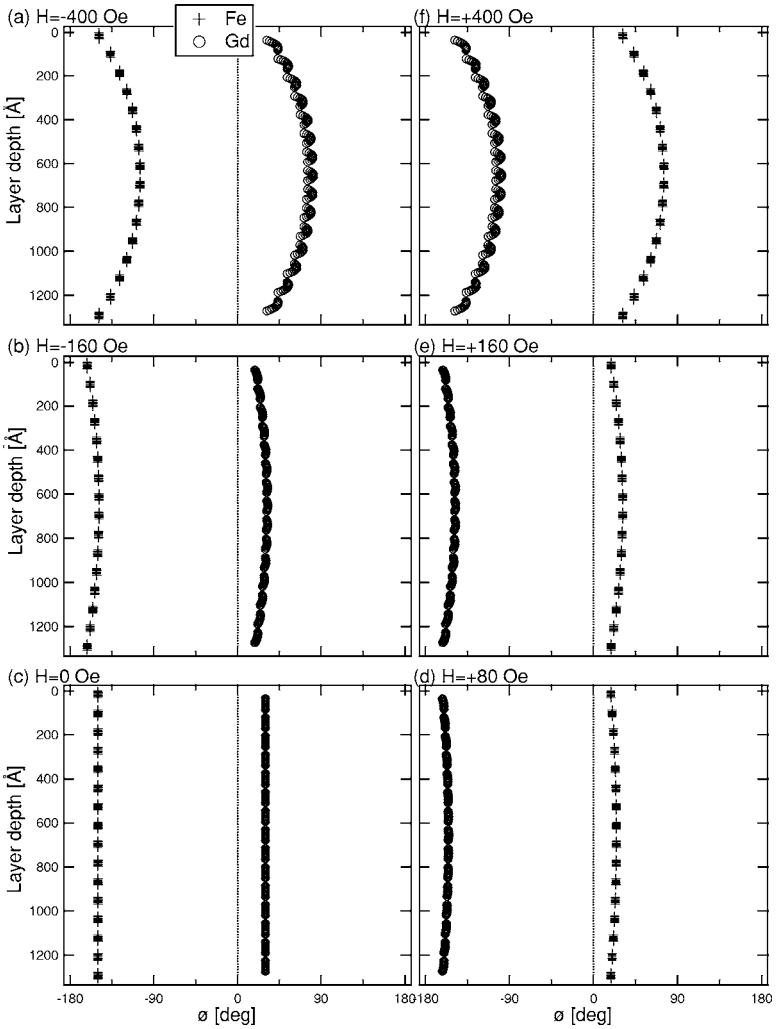

FIG. 7. Spin configurations from simulations for the Fe-terminated sample above T_{Comp} ($T=99$ K) at the selected field values as the field is swept as in Fig. 4. For each sublayer, the magnetization angle ϕ with respect to the applied field direction ($H\|0°$ or $H\|180°$) is plotted as a function of depth from the surface. The circles represent the Gd moments, and the crosses are for the Fe moments. The uniaxial anisotropy of Fe layers is along $\phi=30°$. (a) At −400 Oe, (b) at −160 Oe, (c) at remanence, (d) at +80 Oe, (e) at +160 Oe, and (f) at +400 Oe.

can be explained by these configurations. The XMCD results show that, near T_{Comp}, the total XMCD signals are maximized at zero field and minimized at high fields. The Fe/Gd multilayer is aligned with the anisotropy direction at remanence [Fig. 5(c)], and the Gd and Fe moments spread out across $\phi=\pm 90°$ at high fields [Figs. 5(a) and 5(f)]. This spreading out at high fields occurs in such a way that the total projected moments in the $|\phi|<90°$ and $|\phi|>90°$ regions are nearly equal, hence causing the total Gd- and Fe-XMCD signals to be nearly zero, as shown in the third row in Fig. 3. Even though there are more spins within the $|\phi|<90°$ region, the twisting between spins in the other region is severe enough that the total projected moments are nearly equal for the two regions. The total XMCD hysteresis results also show that the Gd and Fe magnetizations do not change signs even as the applied field is reversed. The simulation results in Fig. 5 agree with the XMCD results showing that the Gd spins are in the $0°<\phi<90°$ region at $H=-160$ and +160 Oe while the Fe spins are in the opposite region [Figs. 5(b) and 5(e)]. However, the direction of the "bulging" is different for the opposite field values. The surface XMCD hysteresis loops from the Fe and Gd layers exhibit a field shift, as shown in Fig. 3, which is also reproduced in the micromagnetic simulations. As the applied field is reversed from −400 to +400 Oe, the Fe and Gd surface-layer moments do not change their signs until $H=+160$ Oe, causing a field shift in the hysteresis loops as if they were biased. The combined effect of the Fe anisotropy and Fe surface termination is evident here. As the field is reversed, a significant field ($\approx+160$ Oe) is required to cant the Fe moments away from the easy axis direction.

The simulation results show $T_{\mathrm{Comp}}\approx 82$ K, and the results follow the trend of the experimental data. Below T_{Comp}, the surface Fe and Gd layer hysteresis loops show twisting at moderate fields, while the total Fe and Gd layer hysteresis loops show slight twisting only at high fields (Figs. 3 and 4). Figure 6 shows the spin configurations at six fields at 41 K. At remanence, the multilayer is in the Gd-aligned state [Fig. 6(c)] and the spins are aligned along the Fe-anisotropy $\mathbf{K_u}$. As the field is increased, twisting starts at the surface and progressively penetrates deeper into the film [Figs. 6(d)–6(f)]. The fanning of spins within a layer is more pronounced in the Gd layer because the exchange coupling of Gd J_{GdGd} is weaker than that of Fe J_{FeFe}. In the surface-twisted state, as shown in Figs. 6(a) and 6(f), the surface layers are magnetized almost perpendicular to the field, while the center layers are magnetized almost collinear with the field.

The experimental and simulation results show that, above T_{Comp} ($T=99$ K), twisting is more pronounced in the total Fe

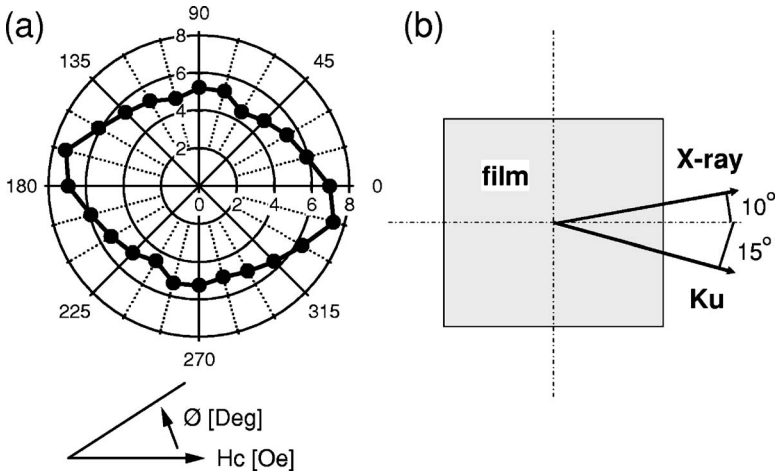

FIG. 8. (a) For the Fe-terminated sample, VSM hysteresis loops are measured at different sample orientations, and coercive fields H_C as a function of the sample orientation are plotted. (b) The anisotropy direction from VSM along with the XMCD measurement direction are shown with respect to the Fe-terminated film.

and Gd hysteresis loops than in the surface Fe and Gd loops (Figs. 3 and 4). This suggests that the moments are more twisted in the interior than in the surface layers, which can be visualized with the spin configuration plots shown in Fig. 7. For $T > T_{\mathrm{Comp}}$, the multilayer is in the Fe-aligned state [Fig. 7(c)] at low fields. As the field is increased, the moments in the middle layers start to twist away from the field direction. The twisting of Gd and Fe moments progresses up to near the surface layer [Figs. 7(d)–7(f)], but the surface layer inhibits the progression of the twisting. The magnetization profile thus becomes inhomogeneous along the depth direction. Because the top Fe layer is aligned parallel to the field, the surface twist does not occur at the surface. In the bulk twisted state, as shown in Figs. 7(a) and 7(f), the moments in the center layers are more twisted away from the field direction than the moments in the surface layers.

As described above, the micromagnetic results match the XMCD experimental data when the anisotropy in the Fe layers was included. To investigate the existence of similar anisotropy in the multilayer samples, hysteresis loop measurements were taken as a function of rotation angle using a vibrating sample magnetometer (VSM). VSM measurements were performed on the Fe-terminated sample at room temperature, and the loops were measured at different in-plane sample orientations. At room temperature, the magnetization contribution from the Gd layers is much smaller compared with that from the Fe layers so that the measured moments are mostly from the Fe layers.[23] The coercive field is plotted as a function of the in-plane orientation in Fig. 8(a) where $\phi = 0°$ corresponds to the case when the applied field is parallel to one of the edges of the rectangular sample. This result indicates that there is some anisotropy in the film, and this uniaxial anisotropy is tilted away from one edge of the sample by approximately 15°.

The exact orientation of the sample's edge with respect to both the x-ray beam and applied magnetic field was determined using the x-ray-irradiation induced surface chemical changes (probably oxidation on Al cap layer[24]) as a reference mark. As shown in Fig. 8(b) the approximate 25° angle between the easy-axis direction determined by VSM and the applied field direction is consistent with the 30° misalignment required to reproduce the effect of anisotropy on the reversal loops near T_{Comp} in the micromagnetic simulations. The origin of the observed uniaxial anisotropy is not clear, but it may be from the film growth process since similar anisotropy is observed in both films that were grown separately.

B. Gd-terminated sample

Similarly measured XMCD hysteresis loops on the Gd-terminated sample are shown in Fig. 9. From the XMCD

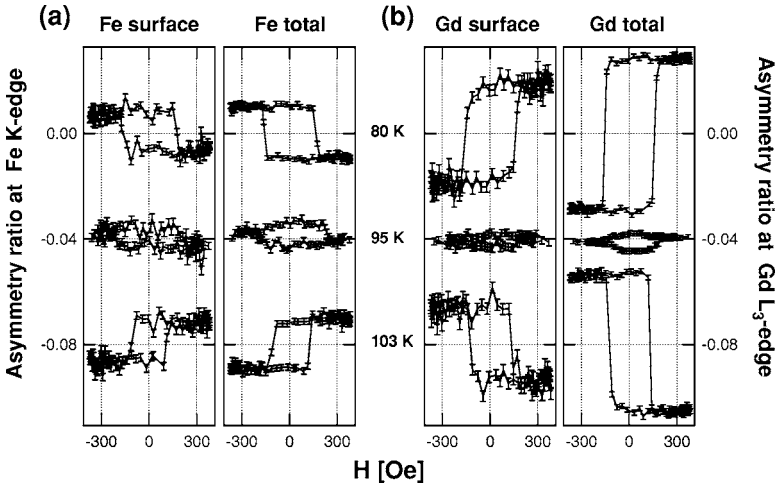

FIG. 9. XMCD hysteresis loops from the Gd-terminated sample at the indicated temperatures. The XMCD signal is recorded as an asymmetry ratio as defined in Sec. II B of the text. The first column in each plot is for the top layers, and the second column is for the total layers. The plots are shifted vertically for clarity. (a) Fe hysteresis loops. (b) Gd hysteresis loops.

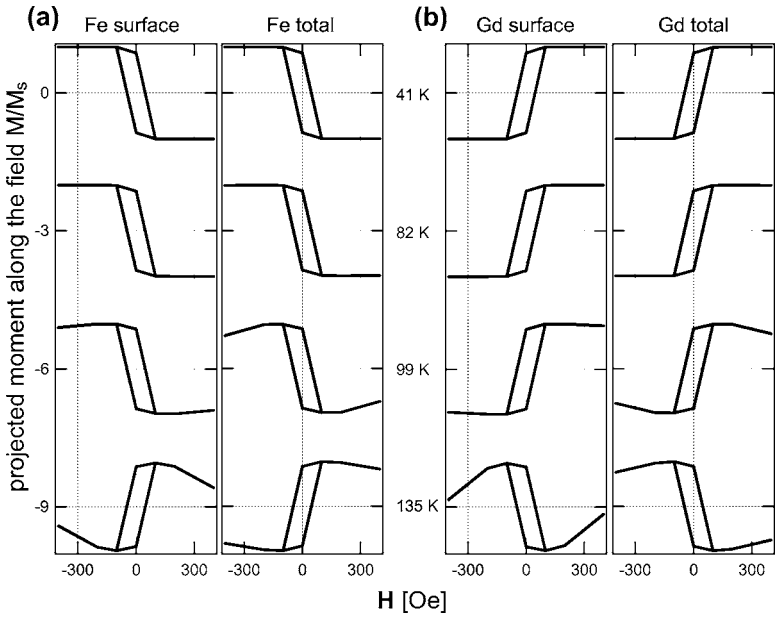

FIG. 10. Micromagnetic simulation on the Gd-terminated multilayer. The plots are shifted vertically for clarity. (a) Fe hysteresis loops. (b) Gd hysteresis loops.

results, T_{Comp} for this sample is near 95 K, consistent with the SQUID results in Fig. 1. The hysteresis loops for $T=95$ K in Fig. 9 show significantly reduced loop heights, in stark contrast with the much larger loop heights obtained below (80 K), and above (103 K) T_{Comp}, respectively. This dramatic reduction in loop height, particularly at high fields where both Gd and Fe sublattices reach nearly zero magnetization, is due to strong canting of Fe and Gd moments towards a 90° direction with the applied field. At T_{Comp}, the Gd/Fe multilayer is nominally an antiferromagnet, and this canting is analogous to a spin-flop transition, as discussed earlier by Camley *et al.*[5]

In contrast to the Fe-terminated sample, the surface-twisted state is not observed in this sample below T_{Comp}. This is expected, since the outermost Gd layers are dominant below T_{Comp} and align with the applied field. Thus an increasing magnetic field stabilizes the Gd aligned phase at the surface. The situation is reversed just above T_{Comp} where the outermost Gd layers are aligned oppositely to the applied field and a surface twist might be expected. However, the numerical calculations of Camley *et al.* on Gd-terminated multilayers show that the transitions into surface- and bulk-twisted states at the moderate fields used here are very close in temperature to each other and to T_{Comp}.[5] The total XMCD loops at 95 K show that the multilayer is in a bulk twisted state and the 5 K step size used in the measurement was too large to discern the closely spaced surface and bulk twisted states in this sample.

The hysteresis loops from the micromagnetic simulations are shown in Fig. 10. The simulation parameters were the same as for the Fe-terminated case, except for the layer stacking sequence. We note that the analysis of x-ray reflectivity data yields a Fe/Gd bilayer thickness somewhat larger than nominal for the Gd-terminated film. Uncertainties in thickness ratio, together with uncertainties in the temperature dependence of Gd magnetization, led to some discrepancy between the measurement and simulation (e.g., T_{Comp} is higher in the simulation, at about 120 K).

It is clear, however, that the extent of twisting is much less pronounced here than in the Fe-terminated case (Fig. 4). Twisting nucleates at higher fields away from T_{Comp}, and at low fields is very significant only in the vicinity of T_{Comp}. This may explain why surface twisting above T_{Comp} was not observed experimentally in the Gd-terminated sample for the limited range of applied fields and 5 K temperature step size used in the measurements (Fig. 9).

IV. SUMMARY AND CONCLUSIONS

Using element-specific and depth-sensitive XMCD measurements, together with micromagnetic simulations, we studied the nucleation and evolution of surface- and bulk-twisted inhomogeneous magnetic states in Fe/Gd multilayers. In addition to clearly observing the surface- and bulk-twisted states predicted long ago by Camley *et al.*,[5] we found that the presence of a small anisotropy has a large effect on the ground state spin configurations attained near the ferrimagnetic compensation temperature T_{Comp}. Away from T_{Comp}, the spin configurations are dictated by the competition between exchange and Zeeman energies. In the absence of significant net magnetization near T_{Comp}, however, the effect of a small anisotropy on the spin configuration becomes evident. Since T_{Comp} can be tuned in $\mathrm{Gd}_{(1-x)}\mathrm{Fe}_x$ alloys to be near room temperature, it is desirable to further study the role of anisotropy in the vicinity of T_{Comp} in this and other artificial ferrimagnetic structures. The unusual reversal loops introduced by the small anisotropy might prove useful in some practical applications for thermomagnetic recording.[25]

ACKNOWLEDGMENTS

The work at Argonne was supported by the U.S. D.O.E., Office of Basic Energy Sciences, under Contract No. W-31-109-ENG-38. We would like to thank C. Karanfil and G. Bunker for help with the bent Laue crystal analyzer.

[1] J. Nogues and I. K. Schuller, J. Magn. Magn. Mater. **192**, 203 (1999); A. E. Berkowitz and Kentaro Takano, *ibid.* **200**, 552 (1999).
[2] S. G. E. te Velthuis, J. S. Jiang, S. D. Bader, and G. P. Felcher, Phys. Rev. Lett. **89**, 127203 (2002); C. Micheletti, R. B. Griffiths, and J. M. Yeomans, Phys. Rev. B **59**, 6239 (1999); F. Keffer and H. Chow, Phys. Rev. Lett. **31**, 1061 (1973).
[3] R. W. Wang, D. L. Mills, Eric E. Fullerton, J. E. Mattson, and S. D. Bader, Phys. Rev. Lett. **72**, 920 (1994).
[4] R. E. Camley and D. R. Tilley, Phys. Rev. B **37**, 3413 (1988).
[5] J. G. LePage and R. E. Camley, Phys. Rev. Lett. **65**, 1152 (1990); R. E. Camley, Phys. Rev. B **35**, 3608 (1987).
[6] Y. Kamiguchi, Y. Hayakawa, and H. Fujimori, Appl. Phys. Lett. **55**, 1918 (1989); H. Fujimori, Y. Kamiguchi, and Y. Hayakawa, J. Appl. Phys. **67**, 5716 (1990); José L. Prieto, Bas B. van Aken, Gavin Burnell, Chris Bell, Jan E. Evetts, Neil Mathur, and Mark G. Blamire, Phys. Rev. B **69**, 054436 (2004).
[7] O. F. K. McGrath, N. Ryzhanova, C. Lacroix, D. Givord, C. Fermon, C. Miramond, G. Saux, S. Young, and A. Vedyayev, Phys. Rev. B **54**, 6088 (1996).
[8] W. Hahn, M. Loewenhaupt, Y. Y. Huang, G. P. Felcher, and S. S. P. Parkin, Phys. Rev. B **52**, 16041 (1995).
[9] N. Ishimatsu, H. Hashizume, S. Hamada, N. Hosoito, C. S. Nelson, C. T. Venkataraman, G. Srajer, and J. C. Lang, Phys. Rev. B **60**, 9596 (1999).
[10] K. Cherifi, C. Dufour, Ph. Bauer, G. Marchal, and Ph. Mangin, Phys. Rev. B **44**, R7733 (1991).
[11] A. Koizumi, M. Takagaki, M. Suzuki, N. Kawamura, and N. Sakai, Phys. Rev. B **61**, R14909 (2000).
[12] D. Haskel, G. Srajer, Y. Choi, D. R. Lee, J. C. Lang, J. Meersschaut, J. S. Jiang, and S. D. Bader, Phys. Rev. B **67**, 180406(R) (2003); D. Haskel, Y. Choi, D. R. Lee, J. C. Lang, G. Srajer, J. S. Jiang, and S. D. Bader, J. Appl. Phys. **93**, 6507 (2003).
[13] D. T. Cromer and D. Liberman, J. Chem. Phys. **53**, 1891 (1970).
[14] J. O. Cross, M. Newville, J. J. Rehr, L. B. Sorensen, C. E. Bouldin, G. Watson, T. Gouder, G. H. Lander, and M. I. Bell, Phys. Rev. B **58**, 11215 (1998).
[15] Y. Choi, D. Haskel, R. E. Camley, D. R. Lee, J. C. Lang, G. Srajer, J. S. Jiang, and S. D. Bader, Phys. Rev. B **70**, 134420 (2004); D. Haskel, G. Srajer, J. C. Lang, J. Pollmann, C. S. Nelson, J. S. Jiang, and S. D. Bader, Phys. Rev. Lett. **87**, 207201 (2001).
[16] L. G. Parratt, Phys. Rev. **95**, 359 (1954); L. Nevot and P. Croce, Rev. Phys. Appl. **15**, 761 (1980).
[17] G. Schütz, W. Wagner, W. Wilhelm, P. Kienle, R. Zeller, R. Frahm, and G. Materlik, Phys. Rev. Lett. **58**, 737 (1987); J. Stöhr, J. Magn. Magn. Mater. **200**, 470 (1999).
[18] J. C. Lang and G. Srajer, Rev. Sci. Instrum. **66**, 1540 (1995).
[19] Zhong Zhong, Dean Chapman, Bruce Bunker, Grant Bunker, Robert Fischetti, and Carlo Segre, J. Synchrotron Radiat. **6**, 212 (1999).
[20] B. L. Henke, E. M. Gullikson, and J. C. Davis, At. Data Nucl. Data Tables **54**, 181 (1993).
[21] A commercial micromagnetics solver by Michael Scheinfein (http://llgmicro.home.mindspring.com).
[22] Bas B. Van Aken, José L. Prieto, and Neil D. Mathur, J. Appl. Phys. **97**, 063904 (2005).
[23] Interfacial Gd magnetization persists above the Gd bulk Curie temperature, see Phys. Rev. Lett. **87**, 207201 (2001).
[24] Any effect due to the possible oxidation layer formation on the cap layer surface was considered negligible. Even if the entire capping layer is Al oxide instead of Al, the critical angle for total external reflection changes only by 15% for both x-ray energies.
[25] S. Tsunashima, J. Phys. D **34**, R87 (2001).